

Melting in metallic Sn nanoparticles studied by surface Brillouin scattering and synchrotron-x-ray diffraction

C. E. Bottani and A. Li Bassi

INFN-Dipartimento di Ingegneria Nucleare, Politecnico di Milano, Via Ponzio 34/3, 20133 Milano, Italy

B. K. Tanner

Department of Physics, University of Durham, South Road, Durham DH1 3LE, United Kingdom

A. Stella and P. Tognini

INFN-Dipartimento di Fisica, "A. Volta," Università degli Studi di Pavia, Via A. Bassi 6, 27100 Pavia, Italy

P. Cheyssac and R. Kofman

Laboratoire de Physique de la Matière Condensée, URA 190, Université de Nice-Sophie Antipolis, 06108 Nice Cedex, France

(Received 21 January 1999)

Brillouin scattering of light off surface acoustic phonons has been used to study the size-dependent melting transition of tin nanocrystals embedded in a silica film on a Si(100) substrate. A jump in the spectral shift of the surface phonon peaks was detected across the melting temperature and the nature of the transition was assessed by the vanishing of Bragg peaks. A simple effective medium treatment of the elastic constants of the film containing solid/liquid inclusions together with a numerical computation of the surface phonon spectrum explains the observed behavior. A strong central peak was also systematically observed just before melting. [S0163-1829(99)51024-2]

Inelastic light scattering has been widely used to study phase transitions.¹ In particular, a great deal of Brillouin work has been dedicated to the freezing of a liquid into the glassy state² and λ phase transitions in allotropic liquids, see, e.g., Alvarenga *et al.*³ Yet, to the best of our knowledge, the melting of a bulk crystal and a nanocrystal (or the freezing of a liquid into an ordered solid phase) was never examined in detail by these techniques.

We report here Brillouin measurements of surface phonons propagating through an amorphous transparent film containing either solid (metallic β tetragonal phase) or liquid tin nanoparticles in a temperature range across the melting temperature for two different nanoparticle sizes: nominally 2.5 nm and 20 nm radius.^{4,5}

The samples were prepared by evaporation condensation of high purity materials in ultrahigh vacuum on silicon substrates. Sn was condensed on a previously evaporated film of SiO_x and the nucleation took place in the liquid state as the substrate was kept at high temperature. After freezing, an additional layer of SiO_x was deposited in order to cover and protect the nanoparticles. This process was repeated many times until the thickness of the layer constituted by Sn particles embedded in a dielectric matrix was about 200 nm. The nanoparticles have the shape of truncated spheres, with a size dispersion lower than 20%.⁴

For both samples the geometry of the system was designed to measure only one phonon peak at a fixed incidence angle. This peak is associated with a modified Rayleigh phonon propagating parallel to the surface and probing both the film and substrate to a depth of the order of 270 nm with the vanishing tail of its displacement field. When the tin particles melt, their shear modulus drops discontinuously to zero and the inverse of their bulk modulus jumps to the value of the

(higher) finite compressibility of the liquid. This corresponds globally to a lowering of the effective elastic constants of the film. Thus the phase velocity of the surface phonon decreases abruptly inducing a redshift in the Brillouin peak position: in this way the melting temperature, which is known to undergo a decrease with size,⁶ can be sharply pinpointed. It is worth noting here that, if the ratio N_s/N (number of atoms on the surface to the total number of atoms) becomes $>10^{-2}$, the melting temperature of the particle starts decreasing down to about $(2/3)T_m$ (melting temperature of the bulk) when N_s/N is about 0.5.⁴ This is expected in terms of application of the Lindeman rule, since the reduced number of bonds on the surface causes an enhancement of thermal vibration. By decreasing the temperature from the liquid state, a supercooling region, due to the existence of typical hysteresis cycles,⁶ is crossed before reaching solidification. The process takes place normally in a temperature range of about 20 K (for instance from 317 to 297 K for particles having radii of about 20 nm).⁴ The hysteresis cycles' reproducibility and electron microscopy data indicate no appreciable presence of residual noncrystalline particles below this region.

At a temperature just below melting, we measured an intense central peak that lowered significantly beyond the melting temperature. In the vicinity of a first-order phase transition one may inspect about this central feature in terms of direct contribution of entropy fluctuations to the dielectric function fluctuations responsible for Brillouin scattering.¹ Yet so far only in the case of bulk scattering in KTaO_3 (Ref. 7) and, at high temperature, in diamond⁸ the central peak could be attributed to scattering from entropy fluctuations in the collision dominated regime. The formal extension of this interpretation to the effective medium consisting of metallic

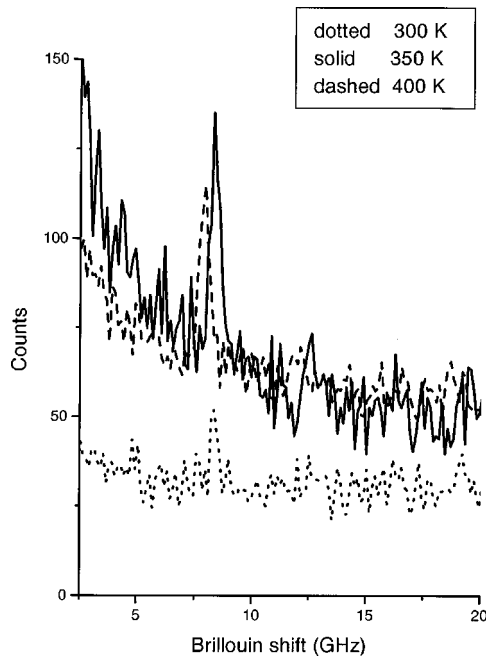


FIG. 1. Experimental Brillouin spectra for the sample with 2.5 nm nominal particle size taken at different temperatures. Mode softening associated with melting (redshift of Rayleigh phonon peak) occurs at 400 K. The rising intensity to the left at 350 K corresponds to the shoulder of an intense central peak centered at 0 GHz.

nanoparticles embedded in a dielectric matrix is not straightforward and is presently in progress.

Surface Brillouin scattering spectra were detected in backscattering at a fixed incidence angle $\theta=70^\circ$ using a Sandercock multipass tandem Fabry-Perot interferometer. The sample was inside an Oxford Instruments cryothermostat Optistat DN-V with optical windows. The spectra were measured at different temperatures in the range 293–600 K with a laser power of 30 mW onto the sample surface. This power was low enough to not significantly enhance the sample temperature. Due to wave-vector conservation, surface phonons contributing to Brillouin scattering have a parallel wavelength $\lambda_{\parallel}=\lambda_0/(2\sin\theta)\approx 274$ nm using the typical laser wavelength $\lambda_0=514.5$ nm of an argon ion laser. Three spectra taken at 300 K, 350 K, and 400 K are shown in Fig. 1. They all are from the film with the smaller particles. On the left of the Rayleigh wave peak a central peak is clearly visible at 350 K, that is, below the melting temperature. Around the melting temperature (≈ 400 K) the central peak is less intense but now softening of the acoustic mode is evident.

As the wavelength λ_{\parallel} of the Rayleigh phonon is much bigger than particle radius it is possible to avoid a detailed description of phonon-particle scattering and treat the film as an effective medium with average elastic properties.

The effective elastic constants B and μ (bulk and shear modulus, respectively) of a film with spherical inclusions, can be obtained within the Voigt-Reuss-Hill approximation⁹ by the formulas

$$B = B_2 - f_1(B_2 - B_1) \frac{3B_2 + 4\mu_2}{3B_1 + 4\mu_2},$$

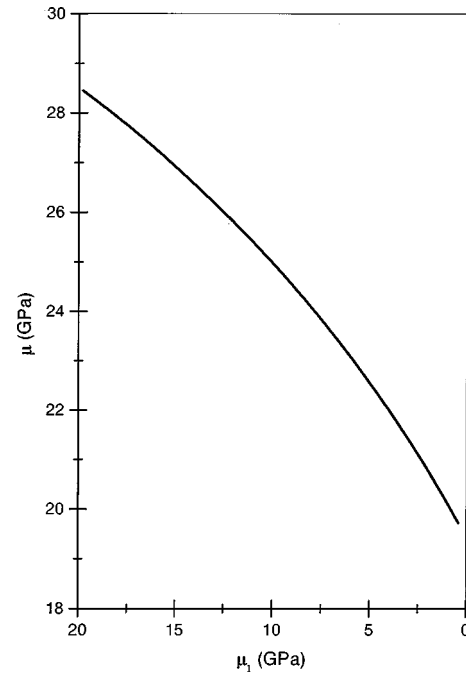


FIG. 2. Effective shear modulus μ of a silica film containing a concentration $f_1=0.2$ of inclusions of shear modulus μ_1 vs μ_1 . For solid Sn nanocrystals $\mu_1=18$ GPa. The minimum of μ is reached when the inclusions are liquid and $\mu_1=0$. For silica $\mu_2=31.2$ GPa and $B_2=36.9$ GPa.

$$\mu = \mu_2 - f_1(\mu_2 - \mu_1) \frac{5(3B_2 + 4\mu_2)}{9B_2 + 8\mu_2 + 6(B_2 + 2\mu_2)\mu_1/\mu_2},$$

where we have neglected the elastic anisotropy of tin particles and 1 stands for tin and 2 for silica (f_1 is the tin

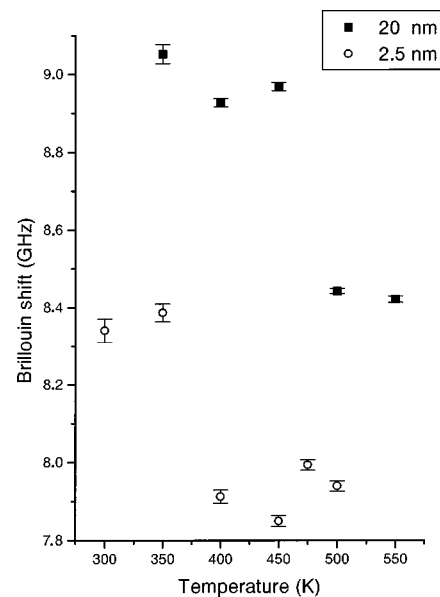


FIG. 3. Rayleigh phonon frequency vs temperature: dots—smaller particles; squares—larger particles. In the latter case the sudden jump in the peak position of 0.6 GHz just across the melting temperature is preceded by a gradual decrease starting from room temperature. Furthermore it is shown that the melting temperature as indicated by Brillouin scattering scales with particle size as expected; that is, smaller particles melt at lower temperatures.

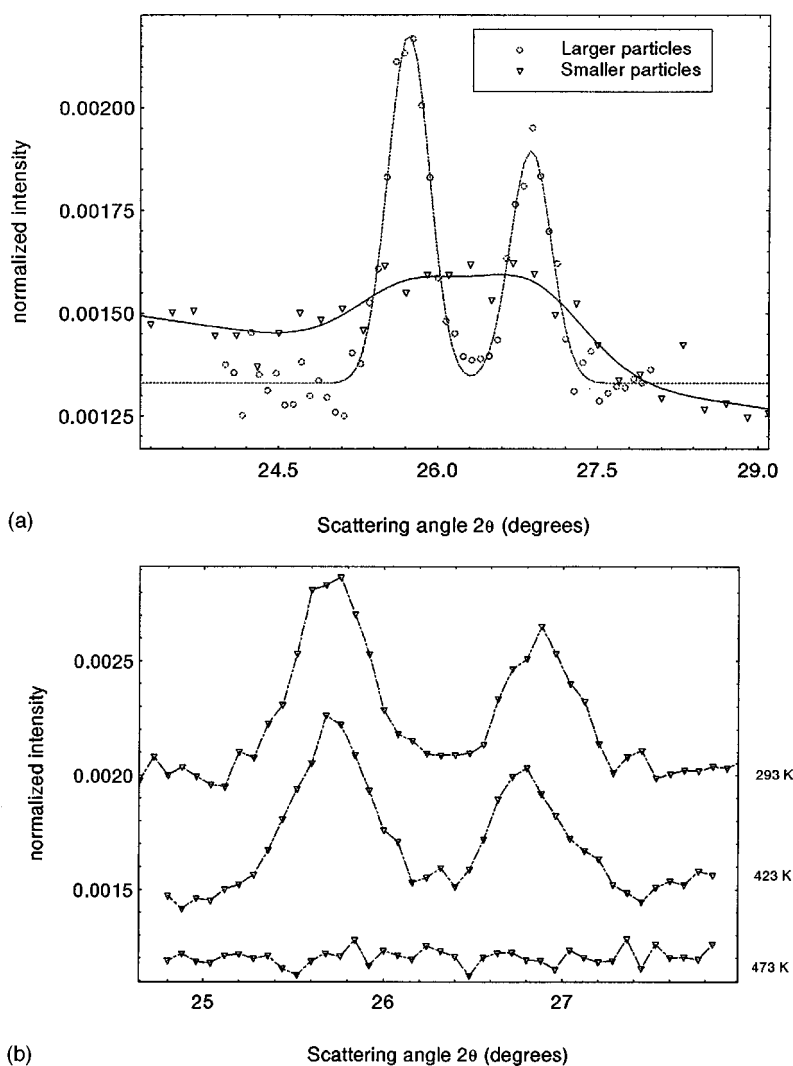


FIG. 4. Bragg peaks of tin nanoparticles: (a) 200 and 101 β -tin peaks in the two samples. Points are the experimental data, solid lines are Gaussian fits to the two peaks. (b) 200 and 101 β -tin peak evolution in the large particle sample.

volume fraction in the film). Figure 2 shows μ as a function of μ_1 . The shear modulus of the film is a minimum when tin is liquid corresponding to $\mu_1 = 0$. As the effect of varying B_1 in the first of the above formulas is negligible, we assume that the main acoustic effect of tin melting is an abrupt lowering of μ , of the order of 35% for our film structure. Computing the surface projected phonon density of states (SPPDS) of the film,^{10,11} we find a redshift of the Rayleigh peak of the order of 1.5 GHz immediately beyond the melting temperature. Experimentally we observed a redshift of about 0.6 GHz (Fig. 3). The agreement roughly within a factor of 2 represents a good test for the interpretation reported above, considering also that (a) the model computation was made using literature values of both tin and silica elastic parameters and that the nominal film deposition geometry was used; (b) effective-medium formulas do not describe particle scattering; and (c) x-ray diffraction (see below) indicates that melting is occurring in the same temperature range as determined from Brillouin scattering.

As Brillouin scattering probes the system at the mesoscopic scale we checked the melting transition directly by measuring the intensities of Bragg peaks of tin nanoparticles.¹² Synchrotron x-ray diffraction was used to

determine the crystallinity of the tin nanoparticles at room temperature and to study their structure as a function of temperature. The diffraction data were collected on the high-resolution powder diffractometer on Station 2.3 at the Synchrotron Radiation Source (SRS) at the Daresbury Laboratory (U.K.). Synchrotron radiation was necessary for the detection of the very weak diffracted intensities scattered from the small tin nanoparticles in the amorphous silica thin film. Following monochromatization using a water-cooled 111 silicon channel cut crystal, the beam was slit collimated to 1 mm \times 4 mm beam. The wavelength chosen, (0.13 nm), was that at which the beam intensity was maximum and the fixed incidence angle, (15°), with respect to the film surface was limited by the geometry of the induction furnace.¹³ A parallel foil Soller slit assembly restricted the angular range of the radiation reaching a Bede Scientific EDRa scintillation detector.¹⁴ Detector scans at room temperature show that the nanoparticles are crystalline and the 200, 101, 220, and 211 peaks of the β -tin tetragonal structure, though very weak, are unambiguously detected, superimposed on a large background. There was very little variation in intensity for specimen scans at fixed scattering angle, showing that the tin crystallites have no preferential orientation. Gaussian profiles can

be fitted to the diffraction peaks and using the Scherrer equation on the full width at half maximum (FWHM) [Fig. 4(a)] yields a particle size of $17 (\pm 1)$ nm for the sample with the larger (20 nm) nominal particle size and $4.5 (\pm 2)$ nm for that with the smaller (2.5 nm) nominal size. As a function of temperature, no significant change was detected in the position of the 200 and 101 peaks (25.76° and 26.915°) in the range 293–423 K. The peaks corresponding to β tin disappeared completely between 423 K and 473 K for the larger particles [Fig. 4(b)] and between 393 K and 423 K for the smaller particles.⁶ No α tin peaks appeared in the diffraction pattern suggesting that melting had occurred, although at temperatures low compared with the melting temperature of bulk tin, which is 505 K. The melting detected by the x-ray diffraction is in the same temperature region as the anomalies in the Brillouin shift and similarly is at a lower temperature for the smaller particle size.

In conclusion, we have shown that Brillouin scattering off surface acoustic phonons can be effectively used to study

nanoparticle melting. The shift of Brillouin peaks shows relevant jumps that allow to determine and pinpoint the size-dependent melting temperature in agreement with x-ray diffraction measurements. Furthermore, a quasielastic (central) peak, the intensity of which reaches a maximum just before melting, has been systematically detected.

Thanks are expressed to T. P. A. Hase and B. D. Fulthorpe for assistance in the x-ray scattering experiments and to A. Mantegazza for technical support in the Brillouin scattering experiments. We acknowledge financial support from “Progetto finalizzato Materiali e Dispositivi per l’Elettronica dello Stato Solido (MADESS II).” C.E.B. and B.K.T. gratefully acknowledge partial financial support from both CRUI (Conferenza dei Rettori delle Università Italiane) and the British Research Council for a joint research program. Provision of synchrotron radiation facilities by the UK EPSRC is acknowledged.

¹W. Hayes and R. Loudon, *Scattering of Light by Crystals* (Wiley, New York, 1978).

²Y. Scheyer, C. Levelut, J. Pelous, and D. Durand, *Phys. Rev. B* **57**, 11 212 (1998).

³A. D. Alvarenga, M. Grimsditch, S. Susman, and S. C. Rowland, *J. Phys. Chem.* **100**, 11 456 (1996).

⁴E. Sondergard, R. Kofman, P. Cheyssac, and A. Stella, *Surf. Sci.* **364**, 467 (1996).

⁵A. Stella, M. Nisoli, S. de Silvestri, O. Svelto, G. Lanzani, P. Cheyssac, and R. Kofman, *Phys. Rev. B* **53**, 15 497 (1996).

⁶A. Stella, P. Cheyssac, R. Kofman, P. G. Merli, and A. Migliori, in *Metastable Phases and Microstructures*, edited by R. Bormann, G. Mazzone, R. D. Shull, R. S. Averback, and R. F. Ziolo, MRS Symposia Proceedings No. 400 (Materials Research Society, Pittsburgh, 1996), p. 101.

⁷K. B. Lyons and P. A. Fleury, *Phys. Rev. Lett.* **37**, 161 (1976).

⁸H. E. Jackson, R. T. Harley, S. M. Lindsay, and M. W. Anderson, *Phys. Rev. Lett.* **54**, 459 (1985).

⁹G. Grimvall, *Thermophysical Properties of Materials* (North-Holland, Amsterdam, 1986), p. 268.

¹⁰G. Ghislotti and C. E. Bottani, *Phys. Rev. B* **50**, 12 131 (1994).

¹¹M. Beghi, C. E. Bottani, P. M. Ossi, T. Lafford, and B. K. Tanner, *J. Appl. Phys.* **81**, 672 (1997).

¹²K. F. Peters, Yip-Wah Chung, and Jerome B. Cohen, *Appl. Phys. Lett.* **71**, 2391 (1997).

¹³C. Tang, G. Bushnell-Wye, and R. J. Cernik, *J. Synchrotron Radiat.* **5**, 929 (1998).

¹⁴S. Cockerton and B. K. Tanner, *Adv. X-Ray Anal.* **38**, 371 (1995).